

Random fragmentation of turbulent molecular clouds lying in the central region of giant galaxies

Suman Paul, Tanuka Chattopadhyay

*Department of Applied Mathematics,
University of Calcutta, 92 A.P.C. Road,
Kolkata 700009*

*Email: spappmath_rs@caluniv.ac.in
tchatappmath@caluniv.ac.in*

Abstract

A stochastic model of fragmentation of molecular clouds has been developed for studying the resulting Initial Mass Function (IMF) where the number of fragments, inter-occurrence time of fragmentation, masses and velocities of the fragments are random variables. Here two turbulent patterns of the velocities of the fragments have been considered, namely, Gaussian and Gamma distributions. It is found that for Gaussian distribution of the turbulent velocity, the IMFs are shallower in general compared to Salpeter mass function. On the contrary, a skewed distribution for turbulent velocity leads to an IMF which is much closer to Salpeter mass function. The above result might be due to the fact that strong driving mechanisms e.g. shocks, arising out of a big explosion occurring at the centre of the galaxy or due to big number of supernova explosions occurring simultaneously in massive parent clouds during the evolution of star clusters embedded into them are responsible for stripping out most of the gas from the clouds. This inhibits formation of massive stars in large numbers making the mass function a steeper one.

Keywords: Molecular clouds, Random fragmentation, Stellar mass spectrum, Turbulence

1. INTRODUCTION

The dynamics of interstellar medium as well as the existence of baryonic dark matter (i.e the matter made of proton and neutron) is closely related to the process of star formation and galaxy evolution. Cool, dense molecular clouds which are fugacious in features, are the key ingredient relative to star formation. The fragmentation occurs due to gravitational collapse of a certain fraction of the molecular cloud when its mass is higher than a critical mass, known as Jeans mass (Jeans [1]) and this continues until the fragmented mass switches over from isothermal to adiabatic phase. Recent studies (Padoan and Nordlund [2], [3]; Machida et al. [4]; Federrath and Klessen [5]; Hopkins [6]; Girat et al. [7]) have shown that gravity and thermal pressure alone are not sufficient to explain star formation, instead turbulence, magnetic field and feedback are the other processes taking active role in star formation. The final stellar mass frequency distribution i.e the Initial Mass Function (hereafter IMF) thus obtained, delivers as the most important tool to study the star formation mechanism. However to find the origin of IMF is still difficult and one of the most profound problems in modern astrophysics.

Salpeter ([8]), in his seminal work, for the first time, showed that the IMF is a single power law distribution for the massive stars of the form, $dN/d\log m \sim m^{-\Gamma}$, for $0.4 M_{\odot} \leq m \leq 10 M_{\odot}$, with index $\Gamma \sim 1.35$, where m is the mass of a star, N denotes the number of stars within some logarithmic mass range m and $m + dm$. In linear mass units, $dN/dm \sim m^{-\alpha}$ makes it possible to estimate the number of stars within the same mass range with $\alpha = \Gamma + 1$. But for the less massive stars, Miller and Scalo ([9]) found that a log normal shape is more likely rather than power law shape. Few years later, the concept of segmented power law was derived (Kroupa et al. [10]; Kroupa [11], [12]) by which the shape of IMF was found to be the joining of two power law segments, one for low mass stars and another for high mass ones. Chabrier ([13], [14], [15]) agreed with the lognormal shape for the low mass stars along with a power law shape above a certain mass ($\sim 0.3 M_{\odot}$) (Larson [16]; Chattopadhyay et al. [17]). Further theoretical and observational works were pursued in this field by many authors like De Marchi et al. ([18]), Zinnecker and Yorke ([19]), Bastian et al. ([20]) and Kroupa et al. ([21]). Collecting data from two satellites Hercules and Leo IV, Geha et al. ([22]) showed that the IMF for the Milky Way is flatter than Kroupa IMF in the high mass regime but consistent with it in the low mass regime. By observing some massive galaxies Smith and Lucey ([23]), Smith et al. ([24]), Newman et al. ([25]) found that these galaxies have IMF consistent with Milky Way IMF but inconsistent with Salpeter or Steeper IMF. The IMFs are most extreme in the central regions of massive galaxies (Martin-Navarro et al. [26]; La Barbera et al. [27]).

Arny ([28]) for the first time has discussed that if the interstellar clouds are predominated by supersonic turbulence (observed by Larson [29]) then the critical mass of gravitational instability is controlled by turbulent velocity rather

than by the temperature. Thus the resulting mass spectrum is determined by interstellar turbulence (Larson [30], [29]; Falgarone et al. [31]). The transient structures of molecular clouds which lead to the fragmentation process are produced mainly due to supersonic turbulent motion (McCrea [32], [33]; Larson [29]), gravitational instability, magnetic field and stellar feedback (Padoan and Nordlund [2]; Machida et al. [4]; Girart et al. [7]). Supersonic turbulence motion for massive stars have vital contribution to describe the theory of hierarchical fragmentation process (Mac Low and Klessen [34]; Krumholz and McKee [35]; Hennebelle and Chabrier [36]; Padoan and Nordlund [3]; Federrath and Klessen [5]; Hopkins [6]).

There are many models to explore the fragmentation process of massive as well as low mass stars but the actual processes are perhaps more complicated as the observational evidences are limited to certain ranges. Considering fragmentation as a random process Elmegreen and Mathieu ([37]) found a log-normal shape to the resulting mass spectrum after four or five iterative steps but inclusion of turbulence (Elmegreen [38]) in this process changed the former shape into a power law form. Chattopadhyay et al. ([39]) considered a time dependent random fragmentation model where Poisson process is taken into account for generating the interoccurrence time between successive fragmentation events and the resulting IMF is a single power law with a steeper slope than Salpeter slope. In all the above models the resulting mass distribution is a single power law which disagrees with the observational evidences which is actually a segmented power law (Kroupa et al. [10]; Kroupa [11], [12]). Chabrier ([13], [14], [15]) also found a mass function which is a combination of a log-normal at lower masses and the Salpeter power law at higher masses. A stochastic model was developed by Chattopadhyay et al. ([17]) for hierarchical fragmentation of molecular cloud using Metropolis-Hastings algorithm which generated the fragment masses and the resulting mass spectrum as a segmented power law that is consistent with observations. The Hierarchical fragmentation process has been discussed recently by many authors (Veltchev et al. [40]; Dobbs et al. [41]; Heyer and Dame [42]; Contreras et al. [43]; Li et al. [44]). From the above discussion it is clear that a proper theory of time dependent random fragmentation predominated by turbulence within molecular clouds may play a significant role in determining the initial mass function (IMF). The present work motivates from the above fact.

In the present work, a time dependent random fragmentation model has been considered in the presence of turbulence having two distinct distributions e.g. Gaussian and Gamma, to investigate how the IMF behaves independently for the molecular cloud mass range $10^3 M_\odot$ to $10^4 M_\odot$ (leading to Open Clusters) and $5 \times 10^4 M_\odot$ to $10^6 M_\odot$ (leading to Globular Clusters) using Monte Carlo technique. Section 2 gives the description of the mathematical model. Section 3 describes numerical simulation, results and discussion. Finally conclusions have been outlined in Section 4.

2. MATHEMATICAL MODEL

2.1. Mass distribution and fragmentation

In the present model, a random hierarchical fragmentation of big turbulent molecular clouds has been considered where, the number of fragments (N_F) formed in each hierarchical step, the interoccurrence time between successive fragmentation (t) in a particular time step of the hierarchy, mass of each fragment (m_f), number of fragmentation steps (n) and turbulent velocity of the fragments (v) are considered as random numbers. The scenario of hierarchical fragmentation of molecular clouds has been first introduced by Hoyle ([45]) and later density inhomogeneity has been observed in several molecular clouds (Meijerink et al. [46]; Schleicher et al. [47]). Subsequent observations show (Sitnik [48]; Schwarz [49]; Song [50]) there is large variation in the masses, ages, structures (continuous or filamentary), turbulence pattern in several molecular clouds observed in different regions of our Galaxy. There is no globally accepted theory so far to explain such variations. Therefore a random fragmentation model has been developed.

The concept of random fragmentation theory was illustrated earlier by many authors (Feller [51]; Elmegreen and Mathieu [37]; Chattopadhyay et al. [39]; Chattopadhyay et al. [17]) to find the model based stellar distribution as a result of fragmentation in a molecular cloud. Elmegreen and Mathieu ([37]) considered a time independent model and took Gaussian distribution for initial distribution of fragments and studied the resulting mass spectrum using Markov Chain Monte Carlo technique. A time dependent random fragmentation model of a rod of length l was considered by Feller ([51]) where he computed that the probability of getting average number of random parts of a total length l , with each part having a length exceeding the length x as,

$$N_F \left(1 - \frac{x}{l}\right)^{N_F-1} \quad (1)$$

where, N_F is the number of random parts while dividing randomly a rod of length l .

Thus if N_F be the total number of fragments formed within a molecular cloud during a given time interval t_1 , the probability that the inter-occurrence time elapsed in successive fragmentations will not exceed t during a particular time step t_1 in the hierarchy, is given by,

$$P(t, N_F, t_1) = 1 - \left(1 - \frac{t}{t_1}\right)^{N_F}, \quad (2)$$

(Chattopadhyay et al. [39]),

where t is a random event following the distribution function,

$$P(t) = 1 - e^{-\lambda t} \quad (3)$$

(Chattopadhyay et al. [39])

and the estimate of $\lambda = \frac{1}{t}$, where, $\bar{t} \leq \frac{y}{n}$, is the average inter-occurrence time

of fragmentation (Chattopadhyay et al. [39]). Here y be the maximum duration of fragmentation in each hierarchical time step and n is the number of fragmentation steps in the hierarchy. Further,

$$n \leq (\log M - \log m_n) / \log N_F, \quad (4)$$

(Chattopadhyay et al. [17]),

where M is the mass of the parent cloud and m_n is the minimum mass of a fragment.

In this work we develop a time dependent random fragmentation model with turbulence as one of the key parameters. For hierarchical fragmentation of the turbulent parent cloud, we generate the fragmented mass by considering the following expression as,

$$m_f \approx \frac{10(T + 100v^2)^{3/2}}{\eta^{1/2}}, \quad (5)$$

(Fleck [52]),

where,

T (in K) is the temperature of the molecular cloud,

η (cm^{-3}) is the number density in the parent cloud,

v (kms^{-1}) is the rms turbulence velocity of a fragment

and m_f (M_\odot) is the mass of a clump after fragmentation.

2.1.1. Turbulent velocity distribution

Due to the stochastic behaviour of turbulence, we choose two distribution nature of turbulence velocity.

1. In the first case we choose a Gaussian distribution for the turbulence velocity which has the following form,

$$N(v)dv = \frac{1}{\sqrt{2\pi}\sigma} e^{-\frac{(v-\mu)^2}{2\sigma^2}} dv, -\infty < v < \infty, \quad (6)$$

(Fleck [52]; Federrath [53]),

where $N(v)dv$ indicates the number density of turbulent fragments within the parent cloud with rms velocities between v and $v + dv$, and μ , σ are population mean and variance.

Here estimate of μ is $\bar{v} = 0.42 \times M_{eff}^{1/5}$ (Larson [29]) is the average value of v and $M_{eff} = \epsilon \times M$, where ϵ is the efficiency of star formation for the parent molecular cloud, $M(M_\odot)$ is the mass of the parent cloud at each fragmentation step and σ is the turbulent velocity dispersion. We set the value of velocity dispersion (σ) as equal to isothermal speed of sound (c_s) (Parker [54]; McCrea [32], [33]) $\sim 0.3 \text{ kms}^{-1}$ (Mach number is unity) (Fleck [52]; Blitz [55]; Williams et al. [56]) in the former case.

In another case we take σ is equal to 1.5 kms^{-1} (Mach number is 5) for

Table 1: values of the parameters

Parameter	value
λ	$\sim 6.5 \times 10^{-5}$
t_1 (years)	~ 300000
$M(M_\odot)$	$10^3 - 10^6$
n	3 , 4
ϵ	0.1 , 0.3
T (K)	10 , 20
$\eta (cm^{-3})$	$10^4 , 5 \times 10^4 , 10^5 , 5 \times 10^5$
$\sigma (kms^{-1})$	0.3, 1.5, 2.4, 3.0
$m_n(M_\odot)$	~ 0.1

Open clusters and 2.4 kms^{-1} (Mach number is 8), 3.0 kms^{-1} (Mach number is 10) for globular clusters (Larson [29]; Schneider et al. [57]; Federrath et al. [58]).

2. In the second case we consider Gamma distribution for turbulence which has the following form,

$$N(v)dv = \frac{\beta^\alpha v^{\alpha-1} e^{-\beta v}}{\Gamma(\alpha)} dv, v > 0, \alpha, \beta > 0, \quad (7)$$

where, α and β are shape and rate parameters respectively. For obtaining α and β we use the following relation,

$$\frac{\alpha}{\beta} = A M_{eff}^{\gamma/2}, \quad (8)$$

(Larson [29]; Chieze [59]; Ossenkopf and Mac Low [60]), where A is a random fraction and $\gamma = 0.3$ (Ossenkopf and Mac Low [60]).

The idea of non Gaussianity arises in the turbulent fluid dynamical models of dissipative system in case of large scale phenomena (Yamamoto and Kambe [61]; Llewellyn Smith and Gille [62]; Pereira et al. [63]) where exponential or skewed Gamma distributions are used. Also violent phenomena involve deviation from Gaussianity e.g. high non Gaussian nature of turbulent velocity in solar flares (Jeffrey et al. [64]).

2.2. Initial choice of different parameters

Here we choose values of a number of parameters to generate fragment masses. The parameters involved in equations (2)-(4) are λ , t_1 , M , m_n and n. For equation (5), the corresponding parameters are temperature (T), turbulent velocity dispersion (σ) and number density of hydrogen molecules in the parent cloud (η).

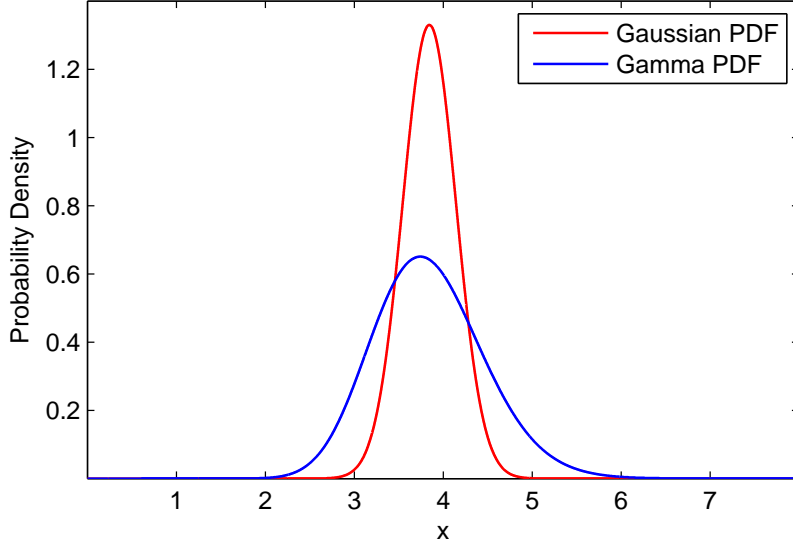


Figure 1: Distinction between two PDFs for the turbulence velocity having mean = 3.845 and standard deviation = 0.3. For Gaussian distribution $\mu = 3.845$, $\sigma = 0.3$ and for Gamma distribution shape parameter $\alpha = 38.45$ and rate parameter $\beta = 10$ i.e. mean = $\frac{\alpha}{\beta} = 3.845$ and standard deviation = $\frac{\alpha}{\beta^2} = 0.3$

Murray and Lin ([65], [66]) asserted that thermal instability in a protoglobular cluster cloud is comparable to the cooling timescale τ_c , where $\tau_c = \frac{3}{2} \frac{kT}{\eta \Lambda(x,t)}$. For a cloud of mass $1.6 \times 10^6 M_\odot$ and number density $\eta = 270 \text{ cm}^{-3}$, $\tau_c = 0.9\tau_d$, τ_d being the dynamical time. So, $\tau_c < \tau_d$. They also showed that the total fragmentation process held on a timescale much shorter than τ_d . For a molecular cloud having number density η , varying in the range $10^4 \text{ cm}^{-3} - 10^6 \text{ cm}^{-3}$ (Herbst and Klemperer [67]; Bally et al. [68], [69]), the dynamical time scale (i.e. free fall time) is of the order 10^5 years – 10^6 years. Hence we have chosen total time of fragmentation (viz. t_1) in that range (viz. Table 1). In our Galaxy we have two types of star clusters, open and globular clusters in the mass regimes $10^2 M_\odot - 10^4 M_\odot$ and $10^4 M_\odot - 10^6 M_\odot$ respectively. Also star clusters are found to be embedded in molecular clouds (Lada and Lada [70]; Yun et al. [71]). Hence the masses of the parent clouds have been considered in the range $10^3 M_\odot - 10^6 M_\odot$. The number of hierarchical fragmentation steps also depends on M (viz. equation (4)). We choose the number of fragmentation steps $n = 3$ for open clusters (Chattopadhyay et al. [39]) and $n = 4$ for globular clusters (Chattopadhyay et al. [17]) and calculate N_F using equation (2) while $t_1 = 300000$ yrs. The minimum fragment mass is taken as $0.1 M_\odot$ ($m_n \sim 0.1 M_\odot$) (Haas and Anders [72]).

In their paper, Goldsmith and Langer ([73]) mentioned that in dense interstellar clouds the kinetic temperatures varied from 10 K to 40 K. Thus temperature used for our model is taken in the above range (viz. Table 1).

The star formation efficiency (SFE) is defined as the fraction of the stellar mass in the star-forming region and the total mass of the parent cloud. (Myers et al. [74]). Federrath and Klessen ([75]), suggested in their work that the range of SFE varies from 0% – 20%. The critical efficiency (ϵ) for molecular clouds have been taken as 0.1 (Federrath and Klessen [75]) and 0.3 (Lada et al. [76]; Rengarajan [77]). All values of the parameters are listed in Table 1.

2.3. Algorithm for numerical simulation

The Cumulative Distribution Function (c.d.f.) for a number of random fragments (N_F) is given by equation (2) when the total number of fragments for a particular time interval (t_1) is known and the mass spectrums are generated following the various steps.

Step 1: Equation (3) can be written in presence of a random fraction k_1 (generated at random from Uniform distribution) as,

$$t = -\frac{1}{\lambda} \log(1 - k_1) \quad (9)$$

Generate one t (random) by putting the value of λ in equation(9).

Step 2: Now equation (2) can be written in the following form as,

$$N_F = \frac{\log(1 - k_2)}{\log(1 - (t/t_1))} \quad (10)$$

where k_2 is a random fraction generated from Uniform distribution. Using the above value of t, we calculate N_F which is the total number of fragments after a fragmentation step.

Step 3: The mass spectrum can be generated using equation (5) for each fragment where the sum of the masses at each fragmentation is equal to the efficient cloud mass ϵM .

Step 4: Similarly we generate second generation mass spectrum for each fragment generated at random during first generation i.e. repeat steps 1 - 4 for each n ($n \sim 3$ or 4).

Finally segmented power laws have been fitted for the generated fragment masses. They are shown in Figures 2 - 4 and Tables 2 - 13.

2.4. Robustness for the segmented power law indices α_1 and α_2

For checking robustness of the results we estimate the values of the slopes for the low mass (viz. $\hat{\alpha}_1$) and high mass (viz. $\hat{\alpha}_2$) ranges following a different model developed by Chattopadhyay et al. ([78]).

The segmented power law distribution for stellar masses is of the form,

$$\frac{dN}{dm} = \begin{cases} Am^{-\alpha_1}, & m_{min} \leq m \leq m_c \\ Bm^{-\alpha_2}, & m_c \leq m \leq m_{max} \end{cases} \quad (11)$$

where, m_{min} and m_{max} are the minimum and maximum masses of the stars, m_c is the characteristic mass at which the turnover occurs, A , B , α_1 and α_2 are constants.

For cross-checking we estimate α_1 in the low mass regime for our generated masses of the fragments, using the following equation as,

$$m_{f_1}^{1-\hat{\alpha}_1} = r_1 m_c^{1-\hat{\alpha}_1} + (1 - r_1) m_{min}^{1-\hat{\alpha}_1}, \quad (12)$$

(Chattopadhyay et al. [78])

Thus, for $r_1 = 0$, $m_{f_1} = m_{min}$ and for $r_1 = 1$, $m_{f_1} = m_{max}$, where, m_{f_1} are the masses generated from equation (5) between m_{min} , m_c and r_1 is a random fraction generated between 0 and 1.

Similarly we estimate α_2 in the high mass regime using the following equation,

$$m_{f_2}^{1-\hat{\alpha}_2} = r_2 m_{max}^{1-\hat{\alpha}_2} + (1 - r_2) m_c^{1-\hat{\alpha}_2}, \quad (13)$$

(Chattopadhyay et al. [78])

Here, when $r_2 = 0$, $m_{f_2} = m_c$ and when $r_2 = 1$, $m_{f_2} = m_{max}$ where, m_{f_2} are the masses generated from equation (5) between m_c and m_{max} and r_2 is a random fraction between 0 and 1.

The estimated values (viz. $\hat{\alpha}_1$ and $\hat{\alpha}_2$) are shown in Tables 4 - 5, Tables 8 - 9 and Tables 12 - 13 (columns 7 - 8 of Tables 4- 5, 8 - 9, 12 - 13 respectively).

3. RESULTS AND DISCUSSIONS

In the present work we have developed a time dependent model of random fragmentation of molecular clouds which is based on the previous works (Feller [51]; Elmegreen and Mathieu [37]; Chattopadhyay et al. [39]; Chattopadhyay et al. [17]) but including turbulence of the fragments arising out of driving mechanisms due to shock waves as a result of explosion in the central region of massive galaxies and other mechanisms e.g. supernova explosions etc. Here a hierarchical fragmentation model has been considered where number of fragments, inter occurrence time of two successive fragmentations, turbulent velocities of the fragments, are all random variables. We have considered two different distributions of turbulent velocity of the fragments, namely, a Gaussian distribution,

which is a symmetric distribution and later a Gamma distribution which is merely a deviation from a symmetric distribution on the basis of two physical mechanisms. When the scale of the driving mechanism is weak, then the velocity is random in its highest mode i.e. the entropy is maximum. Then a Gaussian distribution is suitable for such physical environment. On the contrary when there is a large scale driving mechanism e.g. Galactic shocks, as a result of a big central explosion at its centre or supernova explosions of many massive stars at a time etc. then there is a large deviation from the randomness i.e. the randomness is reduced somewhat and we can consider non Gaussian distributions like Gamma distribution having an entropy which is therefore not a maximum one (Yamamoto and Kambe [61]; Llewellyn Smith and Gille [62]; Pereira et al. [63]; Jeffrey et al. [64]). Hence we have considered these two distributions for the present study. Finally we have computed the mass spectrum in these molecular clouds of various masses and fitted segmented power laws and compared with the observed ones. The following features have been observed.

- For Gaussian distribution of turbulent velocities of the fragments and for the same parent cloud mass, as the efficiency (ϵ) increases, the power laws become flatter in the high mass range for both high and low temperatures. In low mass range it is steeper for low temperature having both low and high efficiencies. In the low mass range it is also steeper for high temperature, low efficiency and flatter for high temperature and high efficiency, for clouds resulting into masses comparable to those of open clusters (Tables 2 and 3). This might be due to the fact that as efficiency increases formation of more massive stars become more frequent making the power law flatter in the high mass range contrary to the reduction of too many low mass fragments turning it to a steeper one. As the temperature increases, for higher efficiency, may be the turbulence is the key parameter which helps to produce low mass fragments in larger numbers perhaps due to elastic collisions among the fragments. Tables 4 - 5 show the estimates of the slopes (viz. $\hat{\alpha}_1, \hat{\alpha}_2$) computed with the model developed by Chatopadhyay et al. ([78]) as a robustness check. These are also consistent with the slopes found using the present model for similar values of the parameters.
- The change in the slopes (viz. α_1, α_2), for clouds leading to open clusters is much higher compared to those leading to globular clusters for a change of efficiency as well as change of the initial temperature of the clouds. Also the values of α_2 are closer to Salpeter index (~ 2.35) in case of clouds forming open clusters than those forming globular clusters. The values of α_1 are much higher than the observed ones ($\sim 0.25-0.3$) in case of open clusters than globular clusters. This leads to the conclusion that formation of massive stars are less likely in open clusters than in globular clusters in general. This is very natural as the masses of globular clusters are largest by almost an order of two in extreme cases. This is to be noted

that the turbulent structure in the present model is Gaussian. The mean value of the turbulence is proportional to the efficient mass of the parent cloud consumed in star formation. As the efficient mass increases (e.g. in case of massive clouds) the mean value of turbulent velocity also increases which is responsible for increasing the mass of the fragment. This in turn produces more massive stars resulting a rather flat mass spectrum in massive star clusters. This fact is in contrast with the case of parent clouds leading to the formation of open clusters of smaller masses.

- It is evident from Figures 2 - 4 and Tables 8 - 9, that with the increase of velocity dispersion ($\sim \sigma$), the resulting mass spectrum has a wider range. This result might be due to the increase of collision rate among the fragments (Field and Saslaw [79], equation III.1) which is responsible for producing a wider range of masses as a result of fragmentation.
- When the turbulent distribution is one of Gamma type (i.e. positively skewed) then the mass functions both for high and low mass ranges of the fragments are comparable to Salpeter slope for high mass end and to the observations (~ 0.3) of low mass stars for various combinations of initial values of the parameters (see Tables 10 - 11). Several authors have pointed out that turbulent velocity deviates from Gaussian distribution (Ossenkopf and Maclow [60]; Krtsuk et al. [80]; Ragot [81]; Federrath et al. [82]; Wilczek et al. [83]; Hennebell and Falgarone [84]; Krumholz and Burkert [85]; Wilczek et al. [86]) due to large scale driving process e.g. shocks produced by supernova explosions (Calzavara and Matzner [87]; Zhang and Chevalier [88]; Sandoval et al. [89]) and other mechanisms e.g. gigantic explosions occurring at the centre of giant galaxies (Miesch and Bally [90]; Sofue ([91], [92]); Mondal and Chattopadhyay [93]). Thus, Gaussian profile of turbulence may be associated with small scale driving mechanism e.g. coalescence and disintegration of fragments (Silk [94]; Silk and Takahashi [95]; Bonnell et al. [96]; Bonnell and Bate [97]), infall of small structures (Takizawa [98]), Active Galactic Nuclei (AGN) Jets (Scannapieco and Brüggen [99]), Galaxy wakes (Roland [100]; Bregman and David [101]; Kim [102]) etc. Hence large scale driving mechanism is responsible for producing open and globular clusters those have mass functions similar to Salpeter type along with a Gamma type turbulence profile but other small scale phenomena are primarily responsible for producing open clusters having Salpeter slope with Gaussian turbulence profile. Gaussian turbulence profile may produce globular clusters in massive clouds but their mass functions will be shallower and vary much from Salpeter mass function (Figer et al. [103]; Stolte et al. [104]; Sung et al. [105]; Kim et al. [106]; Stolte et al. [107]; Harayama et al. [108]; Espinoza et al. [109]). This may be due to the fact that large scale driving mechanism accentuates the escape process of gas from parent clouds leaving little gas for formation of massive stars further which makes the

mass function steeper (e.g. Salpeter type). Thus IMFs in star clusters are not universal but vary from cloud to cloud and from galaxy to galaxy (Dabringhausen et al. [110]; Gunawardhana et al. [111]; Dabringhausen et al. [112]; Marks et al. [113]; Ferreras et al. [114]; Romano et al. [115]) depending on the local or global environments of the parent clouds.

4. CONCLUSION

The present model deals with the turbulent structure of fragments resulting out of time dependent hierarchical fragmentation of molecular clouds lying in the central region of our Galaxy. Two patterns of turbulence have been considered, namely, Gaussian and Gamma distributions. It is found that for a Gaussian distribution, the IMFs are much flatter than Salpeter IMF in the high mass regime and steeper in the low mass regime compared to the observed slopes . On the contrary, the IMFs are comparable to the Salpeter mass function in the high mass regime for a Gamma distribution. The matching is more pronounced in case of initial higher temperature, higher efficiency and for massive parent clouds. The fact may be explained by the driving mechanism prevalent in the environment which originates at the centre of giant galaxies as a result of big central explosion and deviates the pattern of turbulence from a symmetric to one of skewed distributions.

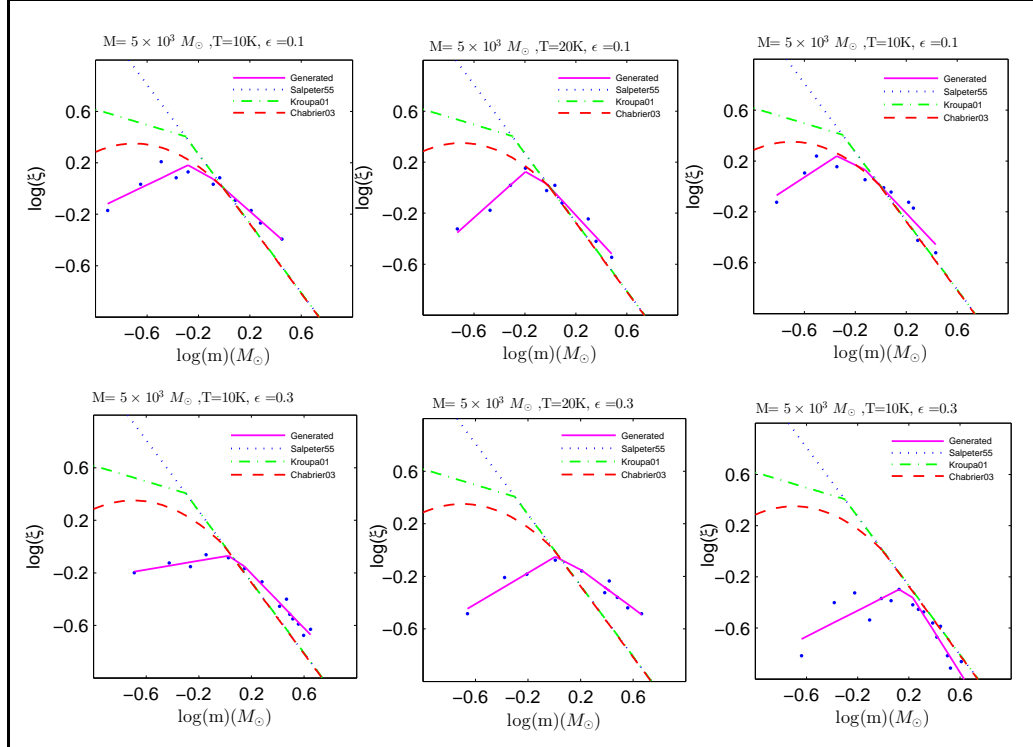


Figure 2: Segmented power law fit for Gaussian distribution of turbulent velocity with $\sigma = 0.3 \text{ kms}^{-1}$ (1st column), $\sigma = 1.5 \text{ kms}^{-1}$ (2nd column) and segmented power law fit for Gamma distribution of turbulent velocity (3rd column) and compared with the observed IMF in the Milky Way by Salpeter ([8]), Kroupa ([11]) and Chabrier ([13])

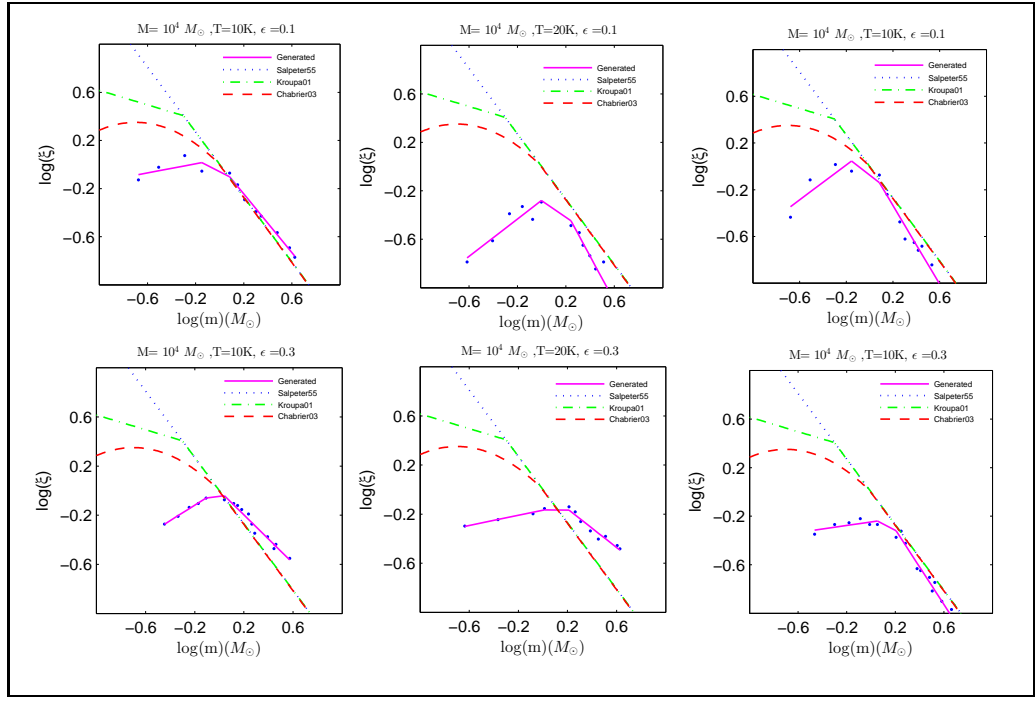


Figure 3: Segmented power law fit for Gaussian distribution of turbulent velocity with $\sigma = 0.3 \text{ km s}^{-1}$ (1st column), $\sigma = 1.5 \text{ km s}^{-1}$ (2nd column) and segmented power law fit for Gamma distribution of turbulent velocity (3rd column) and compared with the observed IMF in the Milky Way by Salpeter ([8]), Kroupa ([11]) and Chabrier ([13])

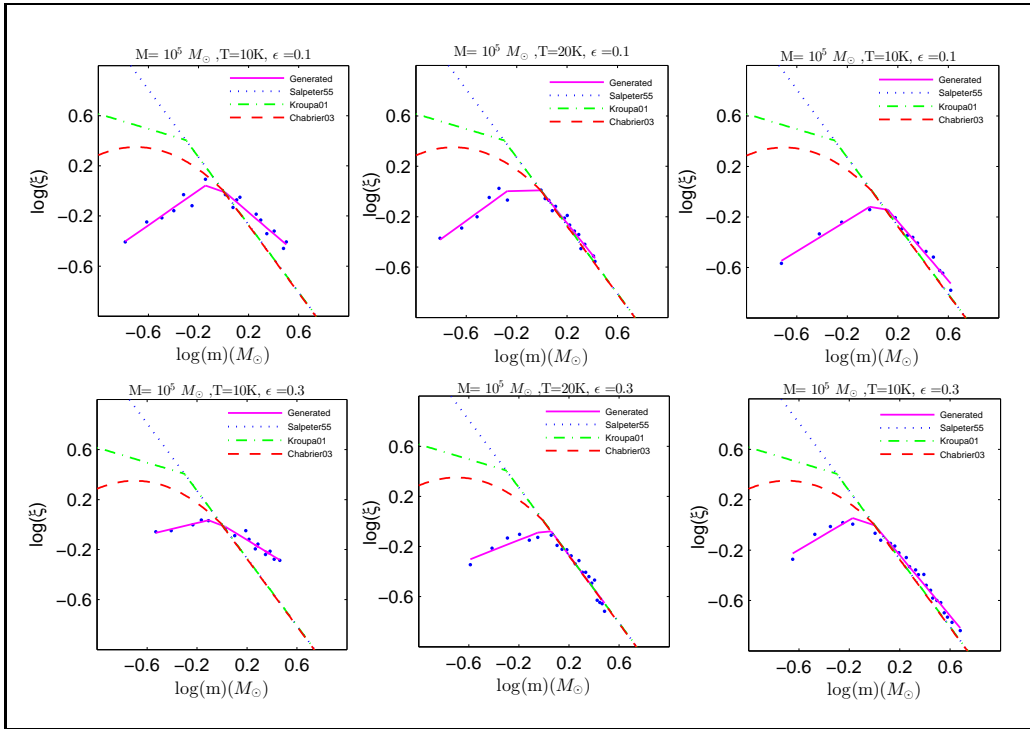


Figure 4: Segmented power law fit for Gaussian distribution of turbulent velocity with $\sigma = 0.3 \text{ kms}^{-1}$ (1st column), $\sigma = 2.4 \text{ kms}^{-1}$ (2nd column) and segmented power law fit for Gamma distribution of turbulent velocity (3rd column) and compared with the observed IMF in the Milky Way by Salpeter ([8]), Kroupa ([11]) and Chabrier ([13])

Table 2: Segmented power-law fit for different initial choices of parameters (leading to open clusters) and for a Gaussian distribution of turbulent velocity

M ($10^4 M_\odot$)	T (K)	ϵ	v (kms^{-1})	η (cm^{-3})	σ (kms^{-1})	N	Γ_1	α_1	Γ_2	α_2
0.1	10	0.1	1.0686	5×10^5	0.3	77	0.4627	0.5373	-0.5343	1.5343
0.1	10	0.3	1.3097	5×10^5	0.3	205	0.4014	0.5986	-1.2822	2.2822
0.1	20	0.1	1.0362	5×10^5	0.3	65	0.3543	0.6457	-0.8725	1.8725
0.1	20	0.3	1.3441	5×10^5	0.3	99	0.1903	0.8097	-1.1106	2.1106
0.5	10	0.1	1.4495	10^5	0.3	226	0.4809	0.5110	-0.8793	1.8793
0.5	10	0.3	1.8169	10^5	0.3	643	0.1680	0.8320	-1.0321	2.0321
0.5	20	0.1	1.4171	10^5	0.3	178	0.3631	0.6369	-1.1553	2.1553
0.5	20	0.3	1.7803	10^5	0.3	436	0.1098	0.8902	-1.1539	2.1539
1	10	0.1	1.7168	10^5	0.3	388	0.1909	0.8091	-1.2197	2.2197
1	10	0.3	2.1389	10^5	0.3	970	0.6296	0.3704	-0.9832	1.9832
1	20	0.1	1.7529	10^5	0.3	359	0.6742	0.3258	-0.9100	1.9100
1	20	0.3	2.1002	10^5	0.3	958	0.2097	0.7903	-1.3906	2.3906

Table 3: Segmented power-law fit for different initial choices of parameters (leading to globular clusters), for a Gaussian distribution of turbulent velocity

M ($10^4 M_\odot$)	T (K)	ϵ	v (kms^{-1})	η (cm^{-3})	σ (kms^{-1})	N	Γ_1	α_1	Γ_2	α_2
5	10	0.1	2.3358	5×10^4	0.3	978	0.4688	0.5312	-0.9345	1.9345
5	10	0.3	2.8744	5×10^4	0.3	3194	0.3160	0.6840	-0.7797	1.7797
5	20	0.1	2.2489	5×10^4	0.3	861	0.6026	0.3974	-0.7654	1.7654
5	20	0.3	2.8209	5×10^4	0.3	2848	0.8081	0.1919	-0.5985	1.5985
10	10	0.1	2.6474	10^4	0.3	1461	0.6938	0.3062	-0.8528	1.8528
10	10	0.3	3.2764	10^4	0.3	7384	0.2397	0.7603	-0.6132	1.6132
10	20	0.1	2.6526	10^4	0.3	1485	0.5547	0.4453	-1.1507	2.1507
10	20	0.3	3.3514	10^4	0.3	7143	0.1254	0.8746	-0.8532	1.8532
50	10	0.1	3.8446	10^4	0.3	6521	0.7824	0.2176	-1.7655	2.7655
50	10	0.3	4.5638	10^4	0.3	34327	0.1188	0.8812	-0.3493	1.3493
50	20	0.1	3.7036	10^4	0.3	5701	0.9192	0.0808	-1.5410	2.5410
50	20	0.3	4.5539	10^4	0.3	29534	0.3807	0.6193	-1.0621	2.0621
100	10	0.1	4.2023	10^4	0.3	11058	0.8870	0.1130	-1.6038	2.6038
100	10	0.3	5.2265	10^4	0.3	62176	0.1260	0.8740	-0.9922	1.9922
100	20	0.1	4.1721	10^4	0.3	10586	0.8825	0.1175	-1.9617	2.9617
100	20	0.3	5.2485	10^4	0.3	56110	0.2862	0.7138	-0.5545	1.5545

Table 4: Estimates for segmented power law indices using truncated Pareto distribution (leading to open clusters), for a Gaussian distribution of turbulent velocity

M ($10^4 M_\odot$)	T (K)	ϵ	m_{min} (M_\odot)	m_c (M_\odot)	m_{max} (M_\odot)	Estimate $\hat{\alpha}_1$ using equation(12)	Estimate $\hat{\alpha}_2$ using equation(13)
0.1	10	0.1	0.1069	0.4669	1.3670	0.3955	1.6123
0.1	10	0.3	0.1510	1.0010	3.1622	0.6033	2.1216
0.1	20	0.1	0.1145	0.4144	1.9123	0.6022	1.4896
0.1	20	0.3	0.4869	1.7100	5.9799	0.7798	1.9842
0.5	10	0.1	0.1242	0.8242	2.8242	0.4593	1.8559
0.5	10	0.3	0.2039	1.3999	4.4596	0.8941	2.1564
0.5	20	0.1	0.2613	1.8613	4.0613	0.5050	1.9965
0.5	20	0.3	0.5940	1.5003	4.2198	0.8998	2.1845
1	10	0.1	0.2106	1.2107	4.2107	0.8137	2.0369
1	10	0.3	0.3570	1.0999	3.7402	0.3654	1.9347
1	20	0.1	0.2872	1.4873	5.0873	0.3321	1.9087
1	20	0.3	0.4162	2.2509	5.9306	0.7996	2.4078

Table 5: Estimates for segmented power law indices using truncated Pareto distribution (leading to globular clusters), for a Gaussian distribution of turbulent velocity

M ($10^4 M_\odot$)	T (K)	ϵ	m_{min} (M_\odot)	m_c (M_\odot)	m_{max} (M_\odot)	Estimate $\hat{\alpha}_1$ from equation(12)	Estimate $\hat{\alpha}_2$ from equation(13)
5	10	0.1	0.2741	2.0241	6.0241	0.4215	2.0069
5	10	0.3	0.6290	1.7701	4.1495	0.7063	1.9989
5	20	0.1	0.5267	2.5268	5.5268	0.5825	1.5926
5	20	0.3	0.4370	1.6998	4.9102	0.2125	1.4657
10	10	0.1	0.1579	1.5677	6.3095	0.6293	2.0154
10	10	0.3	0.3719	1.3399	3.9003	0.7588	1.6544
10	20	0.1	0.2529	2.8028	7.0235	0.4429	2.1985
10	20	0.3	0.4559	1.7100	4.5603	0.7599	1.8049
50	10	0.1	0.5288	2.0290	6.0441	0.3276	2.4795
50	10	0.3	0.2119	1.4893	3.6897	0.7648	1.4578
50	20	0.1	0.5455	4.5023	8.5323	0.2155	2.2666
50	20	0.3	0.5689	1.7575	7.6594	0.6022	2.0001
100	10	0.1	0.5141	4.5143	8.4926	0.1049	2.5491
100	10	0.3	0.3800	2.4700	7.3994	0.8269	1.8999
100	20	0.1	0.5046	1.5046	4.3246	0.4569	1.7445
100	20	0.3	0.5610	1.9601	5.1903	0.7445	1.6987

Table 6: Segmented power-law fit for different initial choices of parameters (leading to open clusters) and for a Gaussian distribution of turbulent velocity

M ($10^4 M_{\odot}$)	T (K)	ϵ	v (kms^{-1})	η (cm^{-3})	σ (kms^{-1})	N	Γ_1	α_1	Γ_2	α_2
0.1	10	0.1	0.8347	5×10^5	1.5	54	0.6325	0.3675	-0.4312	1.4312
0.1	10	0.3	0.9146	5×10^5	1.5	208	0.8823	0.1177	-1.0572	2.0572
0.1	20	0.1	1.4733	5×10^5	1.5	66	0.8127	0.1873	-0.5441	1.5441
0.1	20	0.3	1.3349	5×10^5	1.5	163	0.6527	0.3473	-1.5456	2.5456
0.5	10	0.1	1.5508	10^5	1.5	185	0.7302	0.2698	-1.1995	2.1995
0.5	10	0.3	1.8398	10^5	1.5	565	0.6623	0.3377	-1.0011	2.0011
0.5	20	0.1	0.8338	10^5	1.5	197	0.8956	0.1044	-1.0780	2.0780
0.5	20	0.3	1.7181	10^5	1.5	419	0.5905	0.4095	-0.7385	1.7385
1	10	0.1	1.8454	10^5	1.5	331	0.5100	0.4900	-0.9615	1.9615
1	10	0.3	2.0686	10^5	1.5	534	0.5200	0.4800	-1.1169	2.1169
1	20	0.1	1.6534	10^5	1.5	366	0.7733	0.2267	-1.8515	2.8515
1	20	0.3	1.8822	10^5	1.5	765	0.2074	0.7926	-0.7858	1.7858

Table 7: Segmented power-law fit for different initial choices of parameters (leading to globular clusters), for a Gaussian distribution of turbulent velocity

M ($10^4 M_{\odot}$)	T (K)	ϵ	v (kms^{-1})	η (cm^{-3})	σ (kms^{-1})	N	Γ_1	α_1	Γ_2	α_2
5	10	0.1	2.8604	5×10^4	2.4	1161	0.5562	0.4438	-0.8396	1.8396
5	10	0.3	2.8369	5×10^4	2.4	2683	0.2820	0.7180	-1.0167	2.0167
5	20	0.1	2.1560	5×10^4	2.4	1211	0.5370	0.4630	-1.0423	2.0423
5	20	0.3	2.6290	5×10^4	2.4	2838	0.2378	0.7622	-1.3777	2.3777
10	10	0.1	3.0314	10^4	2.4	2003	0.3365	0.6635	-0.9794	1.9794
10	10	0.3	3.3917	10^4	2.4	5352	0.4618	0.5382	-1.0622	2.0622
10	20	0.1	2.8179	10^4	2.4	1754	0.7214	0.2786	-1.2564	2.2564
10	20	0.3	3.2501	10^4	2.4	5616	0.3939	0.6061	-1.3498	2.3498
50	10	0.1	3.9735	10^4	3.0	6558	0.3020	0.6980	-1.1939	2.1939
50	10	0.3	4.5977	10^4	3.0	30943	0.1289	0.8711	-1.3168	2.3168
50	20	0.1	4.3063	10^4	3.0	6992	0.7727	0.2273	-1.4041	2.4041
50	20	0.3	4.2339	10^4	3.0	28837	0.3706	0.6294	-1.2364	2.2364
100	10	0.1	4.3928	10^4	3.0	13508	0.5877	0.4123	-1.7727	2.7727
100	10	0.3	5.5400	10^4	3.0	66255	0.2787	0.7213	-1.4549	2.4549
100	20	0.1	4.1474	10^4	3.0	11397	0.7308	0.2692	-1.8810	2.8810
100	20	0.3	4.5922	10^4	3.0	53437	0.3173	0.6827	-1.3455	2.3455

Table 8: Estimates for segmented power law indices using truncated Pareto distribution (leading to open clusters), for a Gaussian distribution of turbulent velocity

M ($10^4 M_\odot$)	T (K)	ϵ	m_{min} (M_\odot)	m_c (M_\odot)	m_{max} (M_\odot)	Estimate $\hat{\alpha}_1$ using equation(12)	Estimate $\hat{\alpha}_2$ using equation(13)
0.1	10	0.1	0.1245	0.3725	2.0125	0.3041	1.4229
0.1	10	0.3	0.1217	0.7907	2.6218	0.2054	1.9744
0.1	20	0.1	0.1699	0.4701	2.4299	0.2597	1.5449
0.1	20	0.3	0.2314	1.2314	3.8317	0.3764	2.4897
0.5	10	0.1	0.1038	0.3038	1.4038	0.3009	2.1184
0.5	10	0.3	0.2997	1.6237	4.8977	0.3296	2.1010
0.5	20	0.1	0.1862	0.6363	3.0359	0.2066	1.8746
0.5	20	0.3	0.2180	1.6180	4.8183	0.4115	1.7349
1	10	0.1	0.3270	1.1281	3.7282	0.5039	1.6197
1	10	0.3	0.2609	1.9952	5.2609	0.3926	2.0087
1	20	0.1	0.2427	0.9926	3.9930	0.2311	2.8841
1	20	0.3	0.2311	1.5488	4.2305	0.8080	1.6452

Table 9: Estimates for segmented power law indices using truncated Pareto distribution (leading to globular clusters), for a Gaussian distribution of turbulent velocity

M ($10^4 M_\odot$)	T (K)	ϵ	m_{min} (M_\odot)	m_c (M_\odot)	m_{max} (M_\odot)	Estimate $\hat{\alpha}_1$ from equation(12)	Estimate $\hat{\alpha}_2$ from equation(13)
5	10	0.1	0.1719	0.9219	4.3722	0.4458	1.8013
5	10	0.3	0.4041	2.4043	7.2041	0.7243	2.1145
5	20	0.1	0.2455	0.9454	3.0453	0.3971	2.0421
5	20	0.3	0.3326	2.4547	6.3326	0.7624	2.3269
10	10	0.1	0.1103	2.1101	5.6094	0.5946	1.9332
10	10	0.3	0.4435	2.4434	7.2427	0.4982	2.0358
10	20	0.1	0.3981	1.2181	5.0118	0.7202	2.2128
10	20	0.3	0.3785	1.9512	4.5485	0.6063	2.3941
50	10	0.1	0.3051	2.3052	5.6050	0.5647	2.1865
50	10	0.3	0.3754	2.9512	9.9754	0.8797	2.2388
50	20	0.1	0.5143	3.0143	7.5143	0.2020	2.3142
50	20	0.3	0.4555	3.1622	9.2595	0.6332	2.2719
100	10	0.1	0.3086	2.3086	6.9090	0.3558	2.7576
100	10	0.3	0.4302	2.3434	9.1102	0.6299	2.3188
100	20	0.1	0.9056	4.0056	5.0060	0.1218	2.4651
100	20	0.3	0.5942	2.5002	9.9942	0.6193	2.3019

Table 10: Segmented power-law fit for different initial choice of parameters (leading to open clusters) for Gamma distribution of turbulent velocity

M ($10^4 M_\odot$)	T (K)	ϵ	α	β	v (kms $^{-1}$)	η (cm $^{-3}$)	N	Γ_1	α_1	Γ_2	α_2
0.1	10	0.1	6.029	10	0.6029	5×10^5	63	0.6521	0.3479	-1.0224	2.0224
0.1	10	0.3	13.339	10	1.3339	5×10^5	147	0.2859	0.7141	-1.0143	2.0143
0.1	20	0.1	6.223	10	0.6223	5×10^5	78	0.4527	0.5473	-1.2149	2.2149
0.1	20	0.3	16.286	10	1.6286	5×10^5	201	0.2809	0.7191	-1.3161	2.3161
0.5	10	0.1	12.521	10	1.2521	10^5	249	0.6550	0.3450	-1.0568	2.0568
0.5	10	0.3	17.816	10	1.7816	10^5	520	0.5085	0.4915	-1.5808	2.5808
0.5	20	0.1	7.925	10	0.7925	10^5	193	0.6284	0.3716	-1.6011	2.6011
0.5	20	0.3	15.497	10	1.5497	10^5	633	0.2859	0.7141	-1.5710	2.5710
1	10	0.1	12.458	10	1.2458	10^5	522	0.7488	0.2512	-1.6801	2.6801
1	10	0.3	20.362	10	2.0362	10^5	1115	0.1464	0.8536	-1.5438	2.5438
1	20	0.1	18.216	10	1.8216	10^5	395	0.4510	0.5490	-1.1651	2.1651
1	20	0.3	21.954	10	2.1954	10^5	952	0.5630	0.4370	-1.3916	2.3916

Table 11: Segmented power law fit for different initial choice of parameters (leading to globular clusters) for Gamma distribution of turbulent velocity

M ($10^4 M_\odot$)	T (K)	ϵ	α	β	v (kms $^{-1}$)	η (cm $^{-3}$)	N	Γ_1	α_1	Γ_2	α_2
5	10	0.1	27.621	10	2.7621	5×10^4	1004	0.5677	0.4323	-1.2486	2.2486
5	10	0.3	17.572	10	1.7572	5×10^4	4816	0.4993	0.5007	-1.1989	2.1989
5	20	0.1	25.854	10	2.5854	5×10^4	1236	0.5406	0.4594	-1.4301	2.4301
5	20	0.3	17.216	10	1.7216	5×10^4	3204	0.2638	0.7362	-1.5732	2.5732
10	10	0.1	22.883	10	2.2883	10^4	2110	0.6130	0.3870	-1.1739	2.1739
10	10	0.3	23.753	10	2.3753	10^4	11488	0.5914	0.4086	-1.2022	2.2022
10	20	0.1	19.004	10	1.9004	10^4	1937	0.4719	0.5281	-1.3338	2.3338
10	20	0.3	19.392	10	1.9392	10^4	12717	0.5295	0.4705	-1.3870	2.3870
50	10	0.1	38.457	10	3.8457	10^4	11420	0.8025	0.1975	-1.5242	2.5242
50	10	0.3	31.314	10	3.1314	10^4	31032	0.5049	0.4951	-1.0126	2.0126
50	20	0.1	25.761	10	2.5761	10^4	16967	0.9569	0.0431	-1.6882	2.6882
50	20	0.3	28.470	10	2.8470	10^4	27209	0.5532	0.4468	-1.2696	2.2696
100	10	0.1	36.569	10	3.6569	10^4	20573	0.7127	0.2873	-1.5812	2.5812
100	10	0.3	44.673	10	4.4673	10^4	66296	0.2387	0.7613	-1.4241	2.4241
100	20	0.1	47.131	10	4.7131	10^4	20322	0.9229	0.0771	-1.9393	2.9393
100	20	0.3	31.061	10	3.1061	10^4	55789	0.6318	0.3682	-1.3539	2.3539

Table 12: Estimates for segmented power law indices using truncated Pareto distribution (leading to open clusters), for Gamma distribution of turbulent velocity

M ($10^4 M_\odot$)	T (K)	ϵ	m_{min} (M_\odot)	m_c (M_\odot)	m_{max} (M_\odot)	Estimate $\hat{\alpha}_1$ using equation(12)	Estimate $\hat{\alpha}_2$ using equation(13)
0.1	10	0.1	0.1778	0.3548	1.3182	0.3502	1.9553
0.1	10	0.3	0.2189	1.0025	2.7797	0.7049	2.1265
0.1	20	0.1	0.1584	0.6309	2.1183	0.6321	2.2599
0.1	20	0.3	0.2480	0.8879	2.0897	0.2774	2.2671
0.5	10	0.1	0.1519	0.7519	2.7027	0.3099	2.0374
0.5	10	0.3	0.2299	1.6998	4.8194	0.4905	2.4545
0.5	20	0.1	0.5053	1.5055	3.9057	0.4040	2.5119
0.5	20	0.3	0.4169	1.8399	4.8797	0.7355	2.4220
1	10	0.1	0.2098	0.7009	4.4096	0.2551	2.3974
1	10	0.3	0.3430	1.4501	5.2504	0.9022	2.3142
1	20	0.1	0.3884	1.5885	4.5885	0.5523	2.1114
1	20	0.3	0.6850	1.5599	5.1903	0.5050	2.3189

Table 13: Estimates for segmented power law indices using truncated Pareto distribution (leading to globular clusters), for a Gamma distribution of turbulent velocity

M ($10^4 M_\odot$)	T (K)	ϵ	m_{min} (M_\odot)	m_c (M_\odot)	m_{max} (M_\odot)	Estimate $\hat{\alpha}_1$ from equation(12)	Estimate $\hat{\alpha}_2$ from equation(13)
5	10	0.1	0.3630	2.7631	5.8632	0.4221	2.2613
5	10	0.3	0.2210	1.0997	5.1701	0.4884	2.1006
5	20	0.1	0.3126	1.5125	4.8126	0.3784	2.4447
5	20	0.3	0.6820	2.2202	8.3695	0.7495	2.5729
10	10	0.1	0.3004	2.1003	6.6008	0.3563	2.1465
10	10	0.3	0.2239	1.0099	5.0199	0.3997	2.3119
10	20	0.1	0.3519	2.1522	8.1526	0.5113	2.1653
10	20	0.3	0.2139	0.9590	4.9000	0.4891	2.3557
50	10	0.1	0.6070	2.1071	8.4062	0.2667	2.3362
50	10	0.3	0.3850	1.5399	6.0394	0.4993	2.1147
50	20	0.1	0.2010	1.4018	6.0010	0.0509	2.5792
50	20	0.3	0.5830	2.1399	8.3502	0.3962	2.3161
100	10	0.1	0.6052	1.8050	10.4954	0.2279	2.5883
100	10	0.3	0.5038	1.2589	9.0635	0.7255	2.4301
100	20	0.1	0.6006	2.3998	7.4026	0.2173	2.8181
100	20	0.3	0.4665	1.3970	10.2329	0.3651	2.3559

5. Acknowledgements

The author S.P. is very much grateful to the Department of Science and Technology (DST), India, for approving a JRF grant for the work. The authors are also thankful to A.K.Chattopadhyay for useful discussions. The authors are very much thankful to the referee for valuable suggestions which have improved the work to a great extent.

References

- [1] J. H. Jeans, RSPTA 199 (1902) 1.
- [2] P. Padoan, Å. Nordlund, ApJ 576 (2002) 870.
- [3] P. Padoan, Å. Nordlund, ApJ 730 (2011) 40.
- [4] M. N. Machida, T. Matsumoto, T. Hanawa, K. Tomisaka, MNRAS 362 (2005) 382.
- [5] C. Federrath, R. S. Klessen, ApJ 761 (2012) 156.
- [6] P. F. Hopkins, MNRAS 423 (2012) 2037.
- [7] J. M. Girart, P. Frau, Q. Zhang, et al., ApJ 772 (2013) 69.
- [8] E. E. Salpeter, ApJ 121 (1955) 161.
- [9] G. E. Miller, J. M. Scalo, ApJS 41 (1979) 513.
- [10] P. Kroupa, C. A. Tout, G. Gilmore, MNRAS 262 (1993) 545.
- [11] P. Kroupa, MNRAS 322 (2001) 231.
- [12] P. Kroupa, Science 295 (2002) 82.
- [13] G. Chabrier, PASP 115 (2003a) 763.
- [14] G. Chabrier, ApJL 586 (2003b) 133.
- [15] G. Chabrier, ASSL 327 (2005) 41.
- [16] R. B. Larson, MNRAS 359 (2005) 211.
- [17] T. Chattopadhyay, A. K. Chattopadhyay, A. Sinha, ApJ 736 (2011) 152.
- [18] G. De Marchi, F. Paresce, S. Portegies Zwart, The Initial Mass Function 50 Years Later 327 (2005) 77.
- [19] H. Zinnecker, H. W. Yorke, ARA&A 45 (2007) 481.
- [20] N. Bastian, K. R. Covey, M. R. Meyer, ARA&A 48 (2010) 339.

- [21] P. Kroupa, C. Weidner, J. Pfleiderer-Altenburg, et al., in: Planets, Stars and Stellar Systems Vol. 5, Oswalt, T., Gilmore, G., eds, Springer Netherlands, 2013, p. 115.
- [22] M. Geha, T. M. Brown, J. Tumlinson, et al., *ApJ* 771 (2013) 29.
- [23] R. J. Smith, J. R. Lucey, *MNRAS* 434 (2013) 1964.
- [24] R. J. Smith, P. Alton, J. R. Lucey, C. Conroy, D. Carter, *MNRASL* 454 (2015) 71.
- [25] A. B. Newman, R. J. Smith, C. Conroy, A. Villaume, P. van Dokkum, *ApJ* 845 (2017) 157.
- [26] I. Martín-Navarro, F. La Barbera, A. Vazdekis, J. Falcón-Barroso, I. Ferreras, *MNRAS* 447 (2015) 1033.
- [27] F. La Barbera, A. Vazdekis, I. Ferreras, et al., *MNRAS* 464 (2017) 3597.
- [28] T. Arny, *ApJ* 169 (1971) 289.
- [29] R. B. Larson, *MNRAS* 194 (1981) 809.
- [30] R. B. Larson, *MNRAS* 186 (1979) 479.
- [31] E. Falgarone, T. G. Phillips, C. K. Walker, *ApJ* 378 (1991) 186.
- [32] W. H. McCrea, *RSPSA* 256 (1960) 245.
- [33] W. H. McCrea, in: The Origin of the Solar System, Dermott S. F., eds, Wiley, New York, 1978, p. 75.
- [34] M.-M. Mac Low, R. S. Klessen, *RvMP* 76 (2004) 125.
- [35] M. R. Krumholz, C. F. McKee, *ApJ* 630 (2005) 250.
- [36] P. Hennebelle, G. Chabrier, *ApJL* 743 (2011) 29.
- [37] B. G. Elmegreen, R. D. Mathieu, *MNRAS* 203 (1983) 305.
- [38] B. G. Elmegreen, *ApJ* 486 (1997) 944.
- [39] A. K. Chattopadhyay, T. Kanjilal, B. Basu, *Systems Analysis Modelling Simulation* 43 (2003) 1697.
- [40] T. V. Veltchev, R. S. Klessen, P. C. Clark, *MNRAS* 411 (2011) 301.
- [41] C. L. Dobbs, M. R. Krumholz, J. Ballesteros-Paredes, et al., in: Protostars and Planets VI, Beuther H., Klessen R. S., Dullemond C. P., Henning T., eds, Tucson: Arizona Univ. Press, 2014, p. 3.
- [42] M. Heyer, T. M. Dame, *ARA&A* 53 (2015) 583.

- [43] Y. Contreras, G. Garay, J. M. Rathborne, P. Sanhueza, MNRAS 456 (2016) 2041.
- [44] G.-X. Li, F. Wyrowski, K. Menten, A&A 598 (2017) A96.
doi:10.1051/0004-6361/201628251.
- [45] F. Hoyle, ApJ 118 (1953) 513.
- [46] R. Meijerink, M. Spaans, F. P. Israel, A&A 461 (2007) 793.
- [47] D. R. G. Schleicher, M. Spaans, R. S. Klessen, A&A 513 (2010) 7.
- [48] T. G. Sitnik, Pišma v Astronomicheskii Zhumal 15 (1989) 897.
- [49] K. W. Schwarz, Physical review letters 64 (1990) 415.
- [50] L. Song, Ph.D. thesis, University of Massachusetts,Amherst (2010).
- [51] W. Feller, PhRv 57 (1940) 906.
- [52] R. C. Fleck Jr., MNRAS 201 (1982) 551.
- [53] C. Federrath, MNRAS 436 (2013) 1245.
- [54] E. N. Parker, PhRv 109 (1958) 1328.
- [55] L. Blitz, in: Protostars and Planets III, Levy E. H., Lunine J. I., eds, Tucson: Arizona Univ. Press, 1993, p. 125.
- [56] J. P. Williams, L. Blitz, C. F. McKee, in: Protostars and Planets IV, Mannings V., Boss A. P., Russel S. S., eds, Tucson: Arizona Univ. Press, 2000, p. 97.
- [57] N. Schneider, P. André, V. Könyves, ApJL 766 (2013) 17.
- [58] C. Federrath, J. M. Rathborne, S. N. Longmore, ApJ 832 (2016) 143.
- [59] J. P. Chieze, A&A 171 (1987) 225.
- [60] V. Ossenkopf, M.-M. Mac Low, A&A 390 (2002) 307.
- [61] K. Yamamoto, T. Kambe, Fluid Dynamics Research 8 (1991) 65.
- [62] S. G. Llewellyn Smith, S. T. Gille, Physical Review Letters 81 (1998) 5249.
- [63] R. M. Pereira, C. Garban, L. Chevillard, Journal of Fluid Mechanics 794 (2016) 369.
- [64] N. L. S. Jeffrey, L. Fletcher, N. Labrosse, ApJ 836 (2017) 35.
- [65] S. D. Murray, D. N. C. Lin, ApJ 339 (1989a) 933.
- [66] S. D. Murray, D. N. C. Lin, ApJ 346 (1989b) 155.

- [67] E. Herbst, W. Klemperer, ApJ 185 (1973) 505.
- [68] J. Bally, A. A. Stark, R. W. Wilson, C. Henkel, ApJS 65 (1987) 13.
- [69] J. Bally, A. A. Stark, R. W. Wilson, C. Henkel, ApJ 324 (1988) 223.
- [70] C. J. Lada, E. A. Lada, ARA&A 41 (2003) 57.
- [71] J. L. Yun, A. López-Sepulcre, J. M. Torrelles, A&A 471 (2007) 573.
- [72] M. R. Haas, P. Anders, A&A 512 (2010) A79.
- [73] P. F. Goldsmith, W. D. Langer, ApJ 222 (1978) 881.
- [74] P. C. Myers, P. Dame, T. M. and Thaddeus, et al., ApJ 301 (1986) 398.
- [75] C. Federrath, R. S. Klessen, ApJ 763 (2013) 51.
- [76] C. J. Lada, M. Margulis, D. Dearborn, ApJ 285 (1984) 141.
- [77] T. N. Rengarajan, ApJ 287 (1984) 671.
- [78] T. Chattopadhyay, T. De, B. Warlu, A. K. Chattopadhyay, ApJ 808 (2015) 24.
- [79] G. B. Field, W. C. Saslaw, ApJ 142 (1965) 568.
- [80] A. G. Krtsuk, M. L. Norman, P. Padoan, et al., ApJ 665 (2007) 416.
- [81] B. R. Ragot, ApJ 696 (2009) 1576.
- [82] C. Federrath, J. Roman-Duval, R. S. Klessen, et al., A&A 512 (2010) A81.
- [83] M. Wilczek, A. Daitche, R. Friedrich, Journal of Fluid Mechanics 676 (2011) 191.
- [84] P. Hennebelle, E. Falgarone, A&A Rev. 20 (2012) 55.
- [85] M. R. Krumholz, B. Burkhardt, MNRAS 458 (2016) 1671.
- [86] M. Wilczek, D. G. Vlakov, C. C. Lalescu, in: Progress in Turbulence VII, Springer Proceedings in Physics 196, Örlü, R. et al., eds, Springer International Publishing AG, 2017, p. 3.
- [87] A. J. Calzavara, C. D. Matzner, MNRAS 351 (2004) 694.
- [88] D. Zhang, R. A. Chevalier, MNRAS 482 (2019) 1602.
- [89] M. A. Sandoval, W. R. Hix, O. E. B. Messer, J. A. Harris, E. J. Lentz, AAS 233 (2019) 258.20.
- [90] M. S. Miesch, J. Bally, ApJ 429 (1994) 645.
- [91] Y. Sofue, ApJL 431 (1994) 91.

- [92] Y. Sofue, MNRAS 484 (2019) 2954.
- [93] D. Mondal, T. Chattopadhyay, Bulgarian Astronomical Journal 31 (2019) 16.
- [94] J. Silk, ApJ 143 (1966) 689.
- [95] J. Silk, T. Takahashi, ApJ 229 (1979) 242.
- [96] I. A. Bonnell, M. R. Bate, H. Zinnecker, MNRAS 298 (1998) 93.
- [97] I. A. Bonnell, M. R. Bate, MNRAS 336 (2002) 659.
- [98] M. Takizawa, ApJ 629 (2005) 791.
- [99] E. Scannapieco, M. Brüggen, ApJ 686 (2008) 927.
- [100] J. Roland, A&A 93 (1981) 407.
- [101] J. N. Bregman, L. P. David, ApJ 341 (1989) 49.
- [102] W.-T. Kim, ApJL 667 (2007) 5.
- [103] D. F. Figer, S. S. Kim, M. Morris, et al., ApJ 525 (1999) 750.
- [104] A. Stolte, E. K. Grebel, W. Brandner, D. F. Figer, A&A 394 (2002) 459.
- [105] H. Sung, M. S. Bessell, AJ 127 (2004) 1014.
- [106] S. S. Kim, D. F. Figer, R. P. Kudritzki, F. Najarro, ApJL 653 (2006) 113.
- [107] A. Stolte, W. Brandner, B. Brandl, H. Zinnecker, AJ 132 (2006) 253.
- [108] Y. Harayama, F. Eisenhauer, F. Martins, ApJ 675 (2008) 1319.
- [109] P. Espinoza, F. J. Selman, J. Melnick, A&A 501 (2009) 563.
- [110] J. Dabringhausen, P. Kroupa, H. Baumgardt, MNRAS 394 (2009) 1529.
- [111] M. L. P. Gunawardhana, A. M. Hopkins, R. G. Sharp, et al., MNRAS 415 (2011) 1647.
- [112] J. Dabringhausen, P. Kroupa, J. Pfamm-Altenburg, S. Mieske, ApJ 747 (2012) 72.
- [113] M. Marks, P. Kroupa, J. Dabringhausen, M. S. Pawłowski, MNRAS 422 (2012) 2246.
- [114] I. Ferreras, F. La Barbera, I. G. de La Rosa, et al., MNRASL 429 (2013) 15.
- [115] D. Romano, F. Matteucci, Z.-Y. Zhang, P. P. Papadopoulos, R. J. Ivison, MNRAS 470 (2017) 401.